

# Loss of COMT activity reduces lateral root formation and alters the response to water limitation in sorghum *brown midrib (bmr) 12* mutant

Manny Saluja<sup>1</sup> , Feiyu Zhu<sup>2</sup> , Hongfeng Yu<sup>2</sup> , Harkamal Walia<sup>1</sup>  and Scott E. Sattler<sup>1,3</sup> 

<sup>1</sup>Department of Agronomy and Horticulture, University of Nebraska-Lincoln, Lincoln, NE 68583, USA; <sup>2</sup>Computer Science and Engineering, University of Nebraska-Lincoln, Lincoln, NE 68583, USA; <sup>3</sup>Wheat, Sorghum and Forage Research Unit, USDA-ARS, Lincoln, NE 68583, USA

## Summary

Author for correspondence:

Scott E. Sattler

Email: [scott.sattler@usda.gov](mailto:scott.sattler@usda.gov)

Received: 18 February 2020

Accepted: 22 October 2020

*New Phytologist* (2021) **229**: 2780–2794

doi: 10.1111/nph.17051

**Key words:** *brown midrib*, caffeic acid O-methyltransferase, co-expression analysis, drought response, lateral root, phenylpropanoid metabolism.

- Lignin is a key target for modifying lignocellulosic biomass for efficient biofuel production. *Brown midrib 12 (bmr12)* encodes the sorghum caffeic acid O-methyltransferase (COMT) and is one of the key enzymes in monolignol biosynthesis. Loss of function mutations in COMT reduces syringyl (S) lignin subunits and improves biofuel conversion rate. Although lignin plays an important role in maintaining cell wall integrity of xylem vessels, physiological and molecular consequences due to loss of COMT on root growth and adaptation to water deficit remain unexplored.
- We addressed this gap by evaluating the root morphology, anatomy and transcriptome of *bmr12* mutant. The mutant had reduced lateral root density (LRD) and altered root anatomy and response to water limitation. The wild-type exhibits similar phenotypes under water stress, suggesting that *bmr12* may be in a water deficit responsive state even in well-watered conditions.
- *bmr12* had increased transcript abundance of genes involved in (a)biotic stress response, gibberellic acid (GA) biosynthesis and signaling. We show that *bmr12* is more sensitive to exogenous GA application and present evidence for the role of GA in regulating reduced LRD in *bmr12*.
- These findings elucidate the phenotypic and molecular consequences of COMT deficiency under optimal and water stress environments in grasses.

## Introduction

Plant cells are the major reservoir of photosynthetically fixed carbon, which can be utilized as a renewable energy source for biofuels and renewable chemicals (Kyriakopoulos *et al.*, 2010). Lignin, the second most abundant natural polymer after cellulose, acts as a natural glue and provides mechanical strength to the secondary cell wall structure by cross-linking cell wall components together. The presence of lignin and its hydrophobic properties allows xylem vessels to transport water under negative pressure without collapsing. However, the presence of lignin in secondary cell walls impedes bioenergy conversion processes through saccharification-fermentation (Chen & Dixon, 2007; Dien *et al.*, 2009; Kavousi *et al.*, 2010) and decreases forage digestibility in ruminant livestock (Furtado *et al.*, 2014). Therefore, reducing lignin is a key target for improving bioenergy feedstocks.

Lignin is composed of three major subunits: *p*-hydroxyphenyl (H), guaiacyl (G) and syringyl (S) units derived from phenylalanine through the monolignol pathway of phenylpropanoid metabolism (Vanholme *et al.*, 2013). Loss of function mutations in the genes that encode monolignol biosynthetic enzymes have led to altered H

: G : S ratios, reduced lignin contents and incorporation of atypical subunits into lignin polymers. Mutants or transgenic lines with lower levels of lignin have been isolated in maize, sorghum, pearl millet, rice, Arabidopsis, tobacco, poplar and numerous other species (Vignols *et al.*, 1995; Baucher *et al.*, 1996; Vincent *et al.*, 1997; Baucher *et al.*, 1999; Chabannes *et al.*, 2001; Zhang *et al.*, 2006; Sattler *et al.*, 2010; Cook *et al.*, 2012; Zheng *et al.*, 2017). Mutations at early steps in the monolignol pathway have been associated with collapsed xylem vessels (Jones *et al.*, 2001; Franke *et al.*, 2002). For instance, Arabidopsis *reduced epidermal fluorescence 8 (ref8)* mutant, with a mutated *coumarate 3'-hydroxylase (C3H)* gene, had growth deformities and collapsed xylem elements (Franke *et al.*, 2002). Similarly, *irregular xylem (irx4)* mutant, which contains a mutated *cinnamoyl coenzyme A reductase (CCR)* gene, had partially collapsed xylem vessels in Arabidopsis (Jones *et al.*, 2001). Whereas mutations at early steps drastically reduce monolignol biosynthesis, mutations in the final two steps of the pathway only provoke compositional changes and therefore have little impact on plant fitness (Pincon *et al.*, 2001; Sattler *et al.*, 2009; Ali *et al.*, 2010; Tu *et al.*, 2010; Fu *et al.*, 2011; Sattler *et al.*, 2012; Scully *et al.*, 2016). For instance, sorghum *brown midrib (bmr) 6*

(*cinnamyl alcohol dehydrogenase*, *CAD*) and *bmr12* (*caffeic acid O-methyltransferase*, *COMT*) mutants have significantly altered lignin composition and improved ethanol conversion rates (Dien *et al.*, 2009) with no xylem deformities (Palmer *et al.*, 2008; Sattler *et al.*, 2010).

In addition to its role in plant development, lignin is involved in plant adaptation to abiotic stresses such as drought (Cabane *et al.*, 2012). For instance, increased expression of *CCR* was associated with drought-induced reduction in basal root growth in maize (Fan *et al.*, 2006). Similarly, reduced lignification and spatial shift in *COMT* accumulation was observed in maize leaves under drought stress (Vincent *et al.*, 2005). Mutations in monolignol pathway genes can also alter drought response. For instance, enhanced drought tolerance was observed in *Arabidopsis* phenylalanine ammonia-lyase (*PAL*) double mutant *pal1pal2* (Huang *et al.*, 2010) and in alfalfa *hydroxycinnamoyl CoA:shikimate hydroxycinnamoyl transferase* (*HCT*) antisense line (Gallego-Giraldo *et al.*, 2011). Collectively, these studies suggest that the monolignol pathway plays an important role in drought adaptation (Cesarino, 2019). However, the underlying mechanisms involved in regulating monolignol biosynthesis for drought adaptation are not well-understood.

Drought adaptation is a dynamic process involving continuous physiological and biochemical changes (Harb *et al.*, 2010) and requires higher temporal resolution for better understanding of drought responses. Near range remote sensing platforms (Mir *et al.*, 2012) and nondestructive plant phenotyping using visible, fluorescence and hyperspectral imaging are powerful tools to quantify these dynamic changes at greater temporal resolution (Lazar *et al.*, 2006; Berger *et al.*, 2010; Choat *et al.*, 2019; Khanna *et al.*, 2019).

The sorghum *bmr12-ref* allele has a premature stop codon in the *COMT* gene (Bout & Vermerris, 2003), which changes the composition of lignin deposited in the cell walls, resulting in a drastically higher G : S ratio (Sattler *et al.*, 2012). We examined the *bmr12-ref* root system to understand how compositional changes in lignin affect root growth and response to water deficit. Root morphology and anatomy of *bmr12* were characterized at seedling, vegetative and post-flowering stages under optimal and water limiting conditions. Visible and fluorescence imaging was used to capture temporal growth dynamics and physiological responses of *bmr12* under well-watered (WW) and water-limited (WL) conditions. The molecular basis of altered root growth and its response to water stress was examined using transcriptomics. This study elucidates interactions between monolignol biosynthesis and water stress for modulating plant growth and developmental processes.

## Materials and Methods

### Plant material and seedling stage root system study

Sorghum *COMT* (*bmr12-ref*) and *CAD* (*bmr6-ref*) mutant near isogenic lines in RTx430 background were used for this work (Pedersen *et al.*, 2006). Hereafter, *bmr12-ref* will be referred to as *bmr12*. Maize *COMT* mutant (*bm3*) in AG19 background was obtained from Maize Genetic Cooperation Stock Center,

Champaign, IL, USA. Seedling stage root systems of these lines were evaluated using a cigar roll method (Zhu *et al.*, 2006; Dante *et al.*, 2013; Supporting Information Methods S1).

### Root anatomy and histochemical staining

Wild-type and *bmr12* were grown for 10 days in cigar rolls. A 5 cm root segment was collected from the root–shoot junction and fixed in FAA (90 ml of 70% ethanol : 5 ml of glacial acetic acid : 5 ml 38% formaldehyde) at 4°C, then incubated in a series of ethanol solutions (70%, 60%, 40% and 20%) for 2 h each. Two 1 cm lengths of root tissue were cut from each end of 5 cm root segments and embedded into 8% MetaPhor agarose and sectioned (*c.* 100 µm) using Vibratome 3000 Plus (Leica, Wetzlar, Germany). Further details are provided in Methods S1.

### Nodal root angle measurement

Wild-type and *bmr12* were grown at the University of Nebraska Field Laboratories at Ithaca and Lincoln, NE, USA during the 2017 season. Post-anthesis equally spaced plants (77-days-old) were selected from each row and a soil volume of *c.* 130 ml was excavated, and root stocks were washed clean. Root angles were measured using IMAGEJ software (Abramoff *et al.*, 2004; Methods S1).

### High-throughput visible and fluorescence imaging and analysis

Plant imaging was performed using the LemnaTec 3D Scanalyzer system (LemnaTec GmbH, Aachen, Germany) at Nebraska Innovation Campus, Lincoln, NE, USA. Four seeds of wild-type and *bmr12* were sown in 5.6 l pots (22 cm diameter × 19.5 cm height) filled with 2.5 kg of a soil mix (85% water holding capacity (WHC)) consisting of 188 l compressed peat moss, 170 l vermiculite and 1.4 kg lime. Six days after germination, plants were thinned to one seedling per pot. For the first 21 days, all pots were watered to 85% WHC. After 21 days, for each genotype, water was withheld from five pots (WL), and the other five pots were maintained at 80% WHC (WW). WHC was reduced to 80% so that WW pots are not too wet. Starting from the day water was withheld, WW and WL pots were imaged daily until WL pots reached 30% WHC. Glasshouse conditions were maintained at 28°C : 25°C temperature, 13 h : 11 h, day : night and 40–50% relative humidity. Image processing and trait extraction are detailed in Methods S1.

### Gas exchange measurements

Four replicates of wild-type and *bmr12* were grown under controlled glasshouse conditions and water stress was imposed as described in imaging experiment. After water was withheld, photosynthetic rate and gas exchange were recorded on the newest fully expanded leaf of WW and WL plants at 6, 10 and 17 d using a LI-6800 photosynthesis system (Li-Cor Biosciences, Lincoln, NE, USA). Parameters used for gas exchange measurements are detailed in Methods S1.

## RNA extraction, sequencing and analysis

Whole root tissue was harvested at day 3, 5 and 7 and flash frozen in liquid nitrogen from cigar roll set-up. Three biological replications were used, and each biological replicate consisted of four seedling roots. Frozen samples were ground with a mortar and pestle, 1 ml of TriPure Isolation Reagent (Roche, Basel, Switzerland) was added to each sample, and RNA was extracted following the manufacturer's protocol. RNA sequencing and analysis are detailed in Methods S1. The raw sequencing reads for this study can be found at National Center for Biotechnology Information (NCBI) Sequence Read Archive (SRA) with accession number PRJNA672773.

## First strand cDNA synthesis and reverse transcription quantitative PCR

Reverse transcription quantitative polymerase chain reaction (RT-qPCR) was performed to analyze *COMT* expression in wild-type and *bmr12* roots under WW and WL conditions. The complementary DNA (cDNA) was synthesized in a two-step process using 1 µg of RNA and iScript Reverse Transcription Supermix (Bio-Rad, Hercules, CA, USA). PCR conditions and primer sequences are provided in Methods S1.

## Construction of co-expression network

Weighted Gene Co-expression Network Analysis (WGCNA, v.1.43; Langfelder & Horvath, 2008) was performed to identify gene clusters with similar expression patterns across genotypes, timepoints and treatments. Normalized read counts obtained from DESEQ2 v.1.14.1 (Love *et al.*, 2014) were used to build a gene co-expression network. Parameters used for co-expression network are provided in Methods S1.

## Pharmacological study

Seedlings were grown in cigars rolls for 6 d as described earlier, and Hoagland solution was supplemented with 1, 10 and 100 µM gibberellic acid (GA<sub>3</sub>; G1025; Sigma-Aldrich, St Louis, MO, USA) or 50, 500, 1 and 10 mM daminozide (DMZ; 12033; Cayman Chemical Co., Ann Arbor, MI, USA) or 50, 100, 200, 500 and 1 mM 1-aminocyclopropane-1-carboxylic acid (ACPC; A-3903 Sigma-Aldrich). For each experiment, two batches of three cigar rolls per genotype (total 30 seedlings per genotype) were placed in 1 l beakers. GA was initially dissolved in ethanol and DMZ was dissolved in dimethyl sulfoxide (DMSO). Both solutions were diluted to final concentration with water and the same concentration of ethanol/DMSO was used in all treatments.

## Statistical analysis

Statistical analysis of the results from seedling stage root study, root anatomical, nodal root angle comparison, visible and fluorescence image analysis, gas exchange measurements

and pharmacological study were performed using ANOVA in JMP<sup>®</sup> PRO 13 (SAS Institute Inc., Cary, NC, USA). Tukey's honestly significant difference (HSD) test was used for pair-wise comparisons with an experiment-wise error rate of  $\alpha = 0.05$ .

## Results

### Loss of COMT reduces S lignin deposition in roots

Lignin deposition and *COMT* (*bmr12*) gene expression was examined in *bmr12* roots under WW and WL conditions. Histochemical analysis using Mäule stain, which preferentially stains S lignin subunits, showed reduced deposition of S lignin in *bmr12* roots as compared to the wild-type under both WW and WL conditions (Fig. 1a). Furthermore, RT-qPCR showed 19- and 24-fold lower transcript abundance of *COMT* in *bmr12* seedling roots under WW and WL conditions, respectively (Fig. 1b). The relative transcript abundance of *COMT* was significantly reduced in wild-type when subjected to WL conditions and no further decrease was observed in *bmr12* (Fig. 1b). These results from roots are consistent with previous observations that a nonsense mutation led to reduced expression of *COMT* in vegetative tissues (stalks and leaves) and reduced S lignin concentrations in *bmr12-ref* stover relative to wild-type (Bout & Vermerris, 2003; Palmer *et al.*, 2008; Sattler *et al.*, 2012).

### Loss of COMT leads to reduced lateral root growth and altered root anatomy

To determine the impact of impaired lignin synthesis on root growth under WL conditions, root systems of 6-d-old wild-type and *bmr12* seedlings were examined under WW and WL conditions (Fig. 1c). We did not observe a difference in root length (RL), shoot length (SL) and root : shoot length (RSL) ratio between wild-type and *bmr12* (Table S1). However, lateral root density (LRD) was significantly reduced in *bmr12* under both conditions relative to the wild-type (Fig. 1c). Reduction in LRD could be a consequence of either reduced formation of lateral root primordia (LRP) or failure of LRP to extend beyond the cortex of the primary root. We counted the number of LRP in 6-d-old seedlings under WW conditions and observed significantly reduced LRP density in *bmr12* compared to wild-type (Fig. 1d,e). This result suggested that the reduced LRD in *bmr12* was due to reduced primordia formation. To determine whether this reduced LRD phenotype is unique to *COMT* mutants, the root system of sorghum *CAD* mutant (*bmr6*) was also evaluated, and no significant difference was observed in root morphology between wild-type and *bmr6* (Table S1). This result indicated that loss of *COMT* specifically impacts LRD in sorghum. To address whether the reduction in lateral roots in *COMT* deficient plants is specific to sorghum, we examined the lateral roots in maize *COMT* mutant (*brown midrib3; bm3*) (Fig. S1) (Vignols *et al.*, 1995). Similar to *bmr12* in sorghum, the maize *bm3* also exhibited significantly reduced LRD relative to the wild-type, suggesting

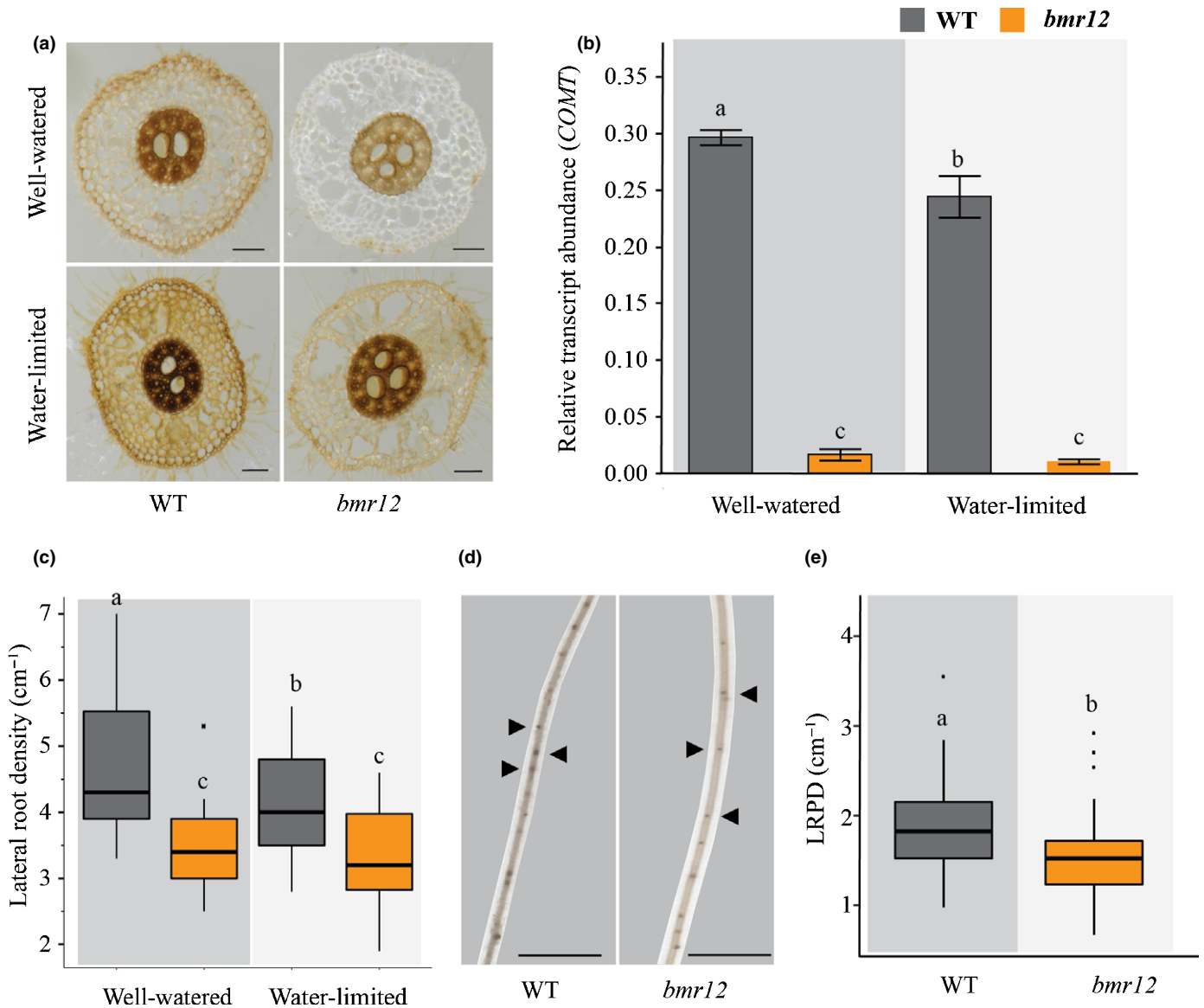


**Fig. 1** Loss of COMT reduces S lignin and lateral root density in sorghum. (a) Mäule staining of root cross sections of 10-d-old RTx430 (wild-type; WT) and sorghum COMT mutant, *bmr12* under well-watered (WW) and water-limited (WL) conditions (bars, 100  $\mu$ m). (b) RT-qPCR analysis of *COMT* in WT and *bmr12* roots under WW and WL conditions ( $n = 6$ ; three biological and two technical replications). Error bars indicate standard error. (c) Lateral root density in 6-d-old WT and *bmr12* under WW and WL conditions ( $n = 30$ ). (d) Representative images of roots showing lateral root primordia in 6-d-old WT and *bmr12* under WW conditions. Black arrows indicate lateral root primordia. Bars, = 250  $\mu$ m. (e) Box plot representing lateral root primordia density (LRPD) in 6-d-old WT and *bmr12* under WW conditions ( $n = 30$ ). In (a–e), 200 ml and 50 ml of one-tenth strength Hoagland solution was used for WW and WL treatment, respectively. The black lines within the boxes marks the median, the upper and lower whiskers represent the first and third quartile of the data, respectively. Outliers are shown as black dots and signify values smaller/greater than first/third quartile, multiplied by 1.5, respectively. For statistical analysis, in (b) and (c) Tukey's test and in (e) Student's *t* test was performed. Different letters indicate significantly different means at  $P < 0.05$ .

that loss of COMT is associated with reduced lateral root number in panicoid grasses.

In addition to reduced LRD, we also observed altered *bmr12* root anatomy (Fig. 2). Under WW conditions, *bmr12* had greater total root, stele, and cortex cross-sectional areas and lower average metaxylem area compared to wild-type. Water limitation resulted in anatomical changes in both wild-type and *bmr12*. Wild-type showed significant increase in total root, stele, and cortex cross-sectional area in response to water limitation and *bmr12*

showed increase in stele and metaxylem area. Taken together, these results indicated that wild-type displayed reduction in LRD and an increase in total root, stele and cortex area when subjected to WL conditions. However, *bmr12* had reduced LRD and increased total root, stele and cortex area as compared to WT under WW conditions which suggested that under WW conditions, (except for metaxylem area) *bmr12* exhibited root phenotypes similar to what wild-type exhibited when subjected to WL conditions.

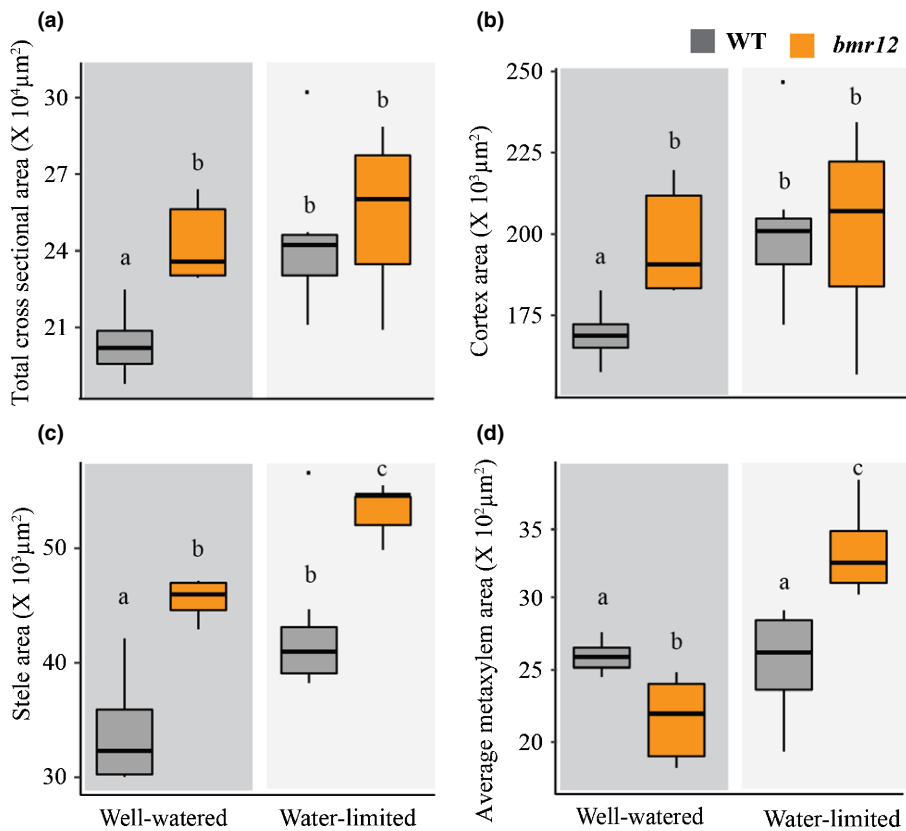


**Fig. 2** Loss of COMT alters root anatomy in sorghum. (a) Total cross-sectional area (b) cortex area, (c) stele area and (d) average metaxylem area in 10-d-old RTx430 (wild-type, WT) and sorghum COMT mutant, *bmr12* under well-watered (WW) and water-limited (WL) conditions. Here, 200 and 50 ml of one-tenth strength Hoagland solution was used for WW and WL treatment. The black lines within the boxes marks the median, the upper and lower whiskers represent the first and third quartile of the data, respectively. Outliers are shown as black dots and signify values smaller/greater than first/third quartile, multiplied by 1.5, respectively. For statistical analysis, Tukey's test was performed and different letters indicate significantly different means at  $P < 0.05$ ,  $n = 10$ .

### Differences in nodal root angle in field grown plants

The sorghum root system has a single embryonic seminal root and multiple post-embryonic nodal roots. To examine whether loss of COMT also affected post-embryonic roots, wild-type and *bmr12* were grown in the field under irrigated and nonirrigated conditions and root systems were excavated to study nodal root architecture from post-anthesis plants. The *bmr12* roots had significantly narrower nodal root angle compared to the wild-type

in both irrigated and nonirrigated field conditions (Fig. 3). This finding suggests that loss of COMT also altered spatial distribution of nodal roots by reducing the nodal root angle in mature plants.

### Image-based temporal response to water stress

Given the alterations in *bmr12* root morphology and anatomy, we next sought to examine whether there is a concomitant change

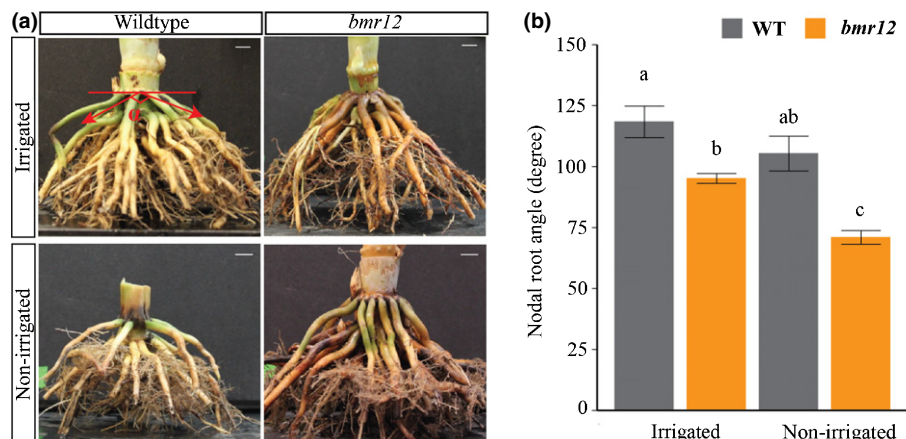


**Fig. 3** Loss of COMT reduces nodal root angle in sorghum. (a) Representative image of RTx430 (wild-type, WT) and *bmr12* root stocks under irrigated (well-watered, WW) and nonirrigated (water-limited, WL) field conditions. Bars, 1 cm. The horizontal red line in top left image represents the axis parallel to the ground surface and two arrows represent the plane of angular spread of nodal roots from the root shoot junction. Nodal root angle (denoted as  $\alpha$ ) was measured in IMAGEJ software (Abramoff *et al.*, 2004). (b) Nodal root angle in WT and *bmr12* under WW and WL field conditions ( $n = 6$ ). For statistical analysis Tukey's test was performed and different letters indicate significantly different means at  $P < 0.05$ . Error bars indicate standard error.

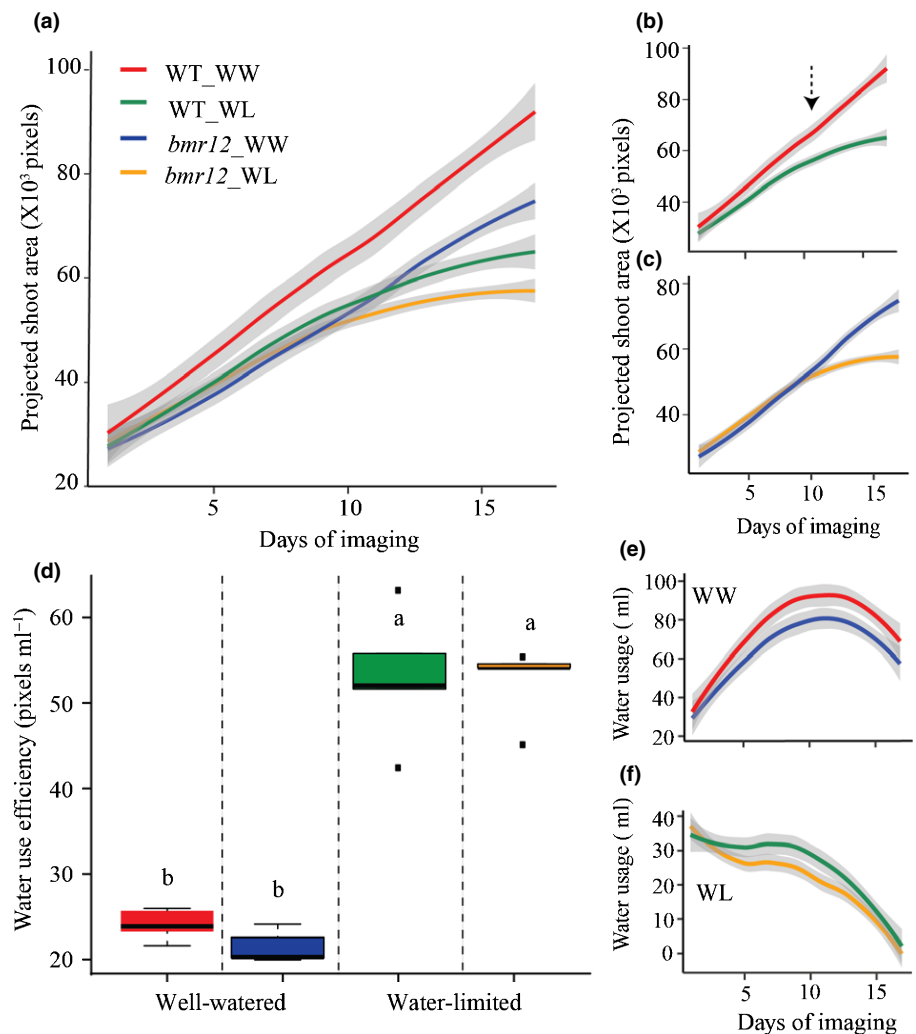
in rate of biomass accumulation and response of *bmr12* to water stress during vegetative growth. We imposed water stress on wild-type and *bmr12* plants by withholding water for 17 days in a glasshouse equipped with automated imaging and watering systems. During this time, soil moisture content decreased from 85% to 30% of soil WHC. Stress induced changes in biomass accumulation were assessed through visible and fluorescence imaging (Campbell *et al.*, 2015) for 17 d, starting from the day water was withheld. To determine the temporal shoot growth differences, 10 red, green and blue (RGB) side view images were obtained for each day and pixel-based traits such as projected shoot area (PSA), plant height, plant width and convex area were calculated. Correlation analysis was performed using four pixel-based traits and four manual biomass related traits, to assess whether pixel-based traits were accurate representations of actual plant biomass and shoot area (Fig. S2). Out of the four pixel-based traits, PSA showed the highest correlation with all four manual biomass related traits and therefore was used to further assess the temporal dynamics of biomass accumulation. A comparison of temporal growth responses of wild-type and *bmr12* plants indicated that the rate of biomass accumulation in *bmr12* is slower than the wild-type under WW conditions (Fig. 4a).

Under WL conditions, wild-type showed higher sensitivity to water-limitation and earlier growth reduction than *bmr12*. Wild-type exhibited significant reduction in PSA in WL conditions as compared to WW conditions starting from day 11 ( $P=0.036$ ) (Fig. 4b). However, *bmr12* was able to maintain shoot growth and did not have a significant reduction in biomass under WL conditions ( $P=0.158$ ; Fig. 4c).

Water limitation had a significant effect on water use efficiency (WUE) (Fig. 4d) and water usage (WU) (Fig. 4e,f) of both genotypes. When subjected to WL conditions, wild-type and *bmr12* used 65.3% ( $P<0.001$ ) and 66.09% ( $P<0.001$ ) less water, compared to their WU under WW conditions, respectively. Although no significant difference in WU and WUE was observed between wild-type and *bmr12* under WW and WL conditions (Fig. 4e,f; Table S2), *bmr12* plants accumulated less biomass than the wild-type.

We also examined the changes in chlorophyll/pigment fluorescence in response to WL treatment. Plants were imaged in a separate chamber for fluorescence, and an ad hoc-image segmentation strategy was used to classify color range of the images into 32 color classes (cc). Pixel-based fluorescence intensity distribution (resolved into multiple cc) changed over time as stress progressed

**Fig. 4** Temporal shoot biomass accumulation and response of RTx430 (wild-type, WT) and sorghum COMT mutant, *bmr12* to water limitation. (a) Comparison of projected shoot area (PSA) between WT and *bmr12* under well-watered (WW) and water-limited (WL) conditions. Reduction in shoot growth in WT (b) and *bmr12* (c) in response to water limitation, where arrow indicates the day of imaging when significant reduction in shoot growth was observed. (d) Comparison of water use efficiency of WT and *bmr12* under WW and WL conditions. (e) Comparison of daily water usage by WT and *bmr12* under WW and WL conditions. For plants under WW treatment, 80% water holding capacity was maintained and water was withheld for WL treatment. The black lines within the boxes marks the median, the upper and lower whiskers represent the first and third quartile of the data, respectively. Outliers are shown as black dots and signify values smaller/greater than first/third quartile, multiplied by 1.5, respectively. For statistical analysis, Tukey's test was performed, and different letters indicate significantly different means at  $P<0.05$ ,  $n=5$ . Solid lines in (a), (b) and (c) represent mean values and shadow indicate standard error.



in the treated plants, and some pixels transitioned from one cc to another due to change in intensity values. To visualize these pixel transitions across the intensity values over time, we performed hierarchical cluster analysis (HCA) for wild-type and *bmr12* under WW and WL conditions (Fig. S3). The clustering analysis resulted in seven distinct clusters that we labeled I–VII (Fig. S3). Clusters II and VI, the two largest clusters are almost entirely populated by wild-type and *bmr12* WL and *bmr12* WW derived distributions (Fig. 5). In contrast, cluster VII is specific to wild-type WW treatment, further supporting the hypothesis that *bmr12* WW plants exhibited image-derived signatures that were similar to the wild-type WL, which were resolved through clustering for most wild-type WW plants especially from 8 to 14 d range (Fig. 5). The temporal context of *bmr12* WW plants showing a more similar response pattern to stressed plants is evident during early stages (1–5 d, cluster II) and mid-to-later stages (8–17 d, cluster VI) of the experiment. Further, our analysis also identified cluster V from the fluorescence signal of cc 8 and 9 to be specific to WL conditions only (day 13 and 14) for both wild-type and *bmr12* (Fig. S3). Collectively, visible and fluorescence imaging suggest that *bmr12* under WW conditions responded similarly to wild-type under WL conditions on a temporal scale.

#### Assessing changes in gas exchange properties in response to water deficit

We next examined the physiological response of the two genotypes under WW and WL conditions at three time points (6, 10 and 17 d) by measuring the gas exchange parameters (Fig. S4).

For WL treatment water was withheld for 17 d from 21-d-old plants. Water stress significantly altered CO<sub>2</sub> assimilation rate (*A*), transpiration rate (*E*) and stomatal conductance (*gsu*) in both the genotypes. Both genotypes exhibited a significant decrease in the CO<sub>2</sub> assimilation rate under WL conditions only on day 17 (wild-type:  $P=0.028$ ; *bmr12*:  $P=0.0005$ ) (Fig. S4). There were no significant differences in CO<sub>2</sub> assimilation rate between wild-type and *bmr12* under WW and WL conditions. Under WL conditions, *bmr12* displayed reduction in stomatal conductance earlier than wild-type ( $P=0.0160$ , Fig. S4). This result suggests that *bmr12* leaves might be more responsive to water stress, and consequently may adjust their stomatal conductance earlier than the wild-type leaves.

#### Network analysis identified differential transcriptional regulation in *bmr12*

Next, we examined the impact of loss of COMT function on the transcriptome of *bmr12* roots at 3, 5 and 7 days under WW and WL conditions and the results were compared to wild-type seedlings under the same conditions. Based on our transcriptome analysis, 86–90% of the sequencing reads were uniquely aligned to the reference genome and 126, 213, 229 genes were differentially expressed (false discovery rate (FDR) < 0.05) in WW and 152, 226, 289 genes in WL conditions on day 3, 5 and 7, respectively, between wild-type and *bmr12* (Table S3). Differential expression of several genes between wild-type and *bmr12* suggested that loss of COMT resulted in transcriptional changes in *bmr12* under both WW and WL. Next, we performed weighted

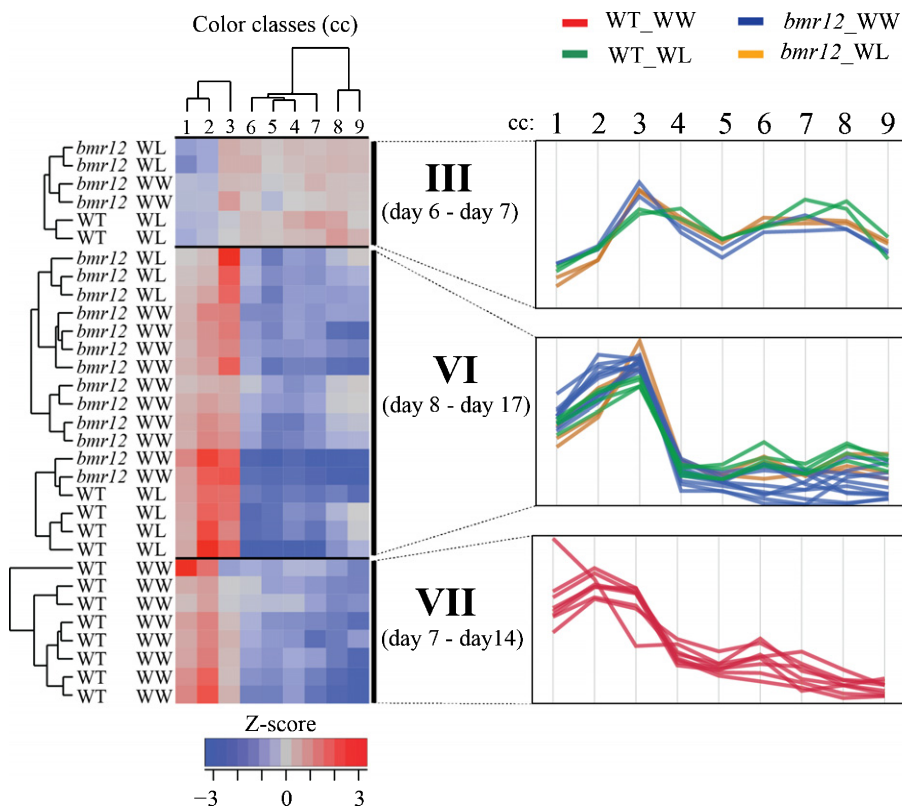


**Fig. 5** Sorghum COMT mutant, *bmr12* exhibits drought induced fluorescence signature under well-watered (WW) conditions. Hierarchical cluster analysis was performed using standardized Z-scores for pixel counts (normalized to plant size) for color classes (cc) for genotype, treatment and day following Wards method in JMP® pro 13. Heatmap represents normalized pixel count for each color class clustered by genotype (RTx430 (wild-type, WT) and *bmr12*), treatment (well-watered (WW) and water limited (WL)) and days of imaging. Roman numerals (III, VI and VII) on the right of heatmap represents cluster numbers with days of imaging mentioned in parenthesis. The line plots on the right represents the parallel coordinate plot for each cluster. WT\_WW, wild-type under WW conditions; WT\_WL, wild-type under WL conditions; *bmr12*\_WW, *bmr12* under WW conditions; *bmr12*\_WL, *bmr12* under WL conditions. Color key represents the standardized Z-score values.

gene co-expression analysis (WGCNA) on whole transcriptome, which yielded 29 modules (ME) representing genes with differential co-expression patterns across genotypes, treatments and days (Fig. S5; Table S4). Out of 29 modules, two modules (ME15 and ME21) were associated with response to water deficit. ME15 consisted of genes with higher transcript levels under WW conditions and ME21 contained genes with higher transcript levels under WL conditions. In addition, there were three modules associated with constitutively higher gene expression in either *bmr12* (ME9 and ME20) or wild-type (ME10) under both WW and WL conditions. ME9, ME10 and ME20 containing 76, 43 and 41 differentially expressed genes (DEGs) (log fold change > 1, FDR < 0.05), respectively, were further examined to identify transcriptional differences between *bmr12* and wild-type. Gene ontology (GO) analysis of DEGs showed enrichment for GO terms related to transport (GO:006810), localization (GO:0051179), establishment of localization (GO:0051234) in ME9 and heme-binding (GO:0020037) and tetrapyrrole binding (GO:0046906) in ME10. No significant GO enrichment was observed in ME20. Some DEGs in these modules were involved in phenylpropanoid pathway, various stress responses and hormone biosynthesis and signaling (Fig. 6).

### Expression of lignin related genes was altered due to loss of COMT

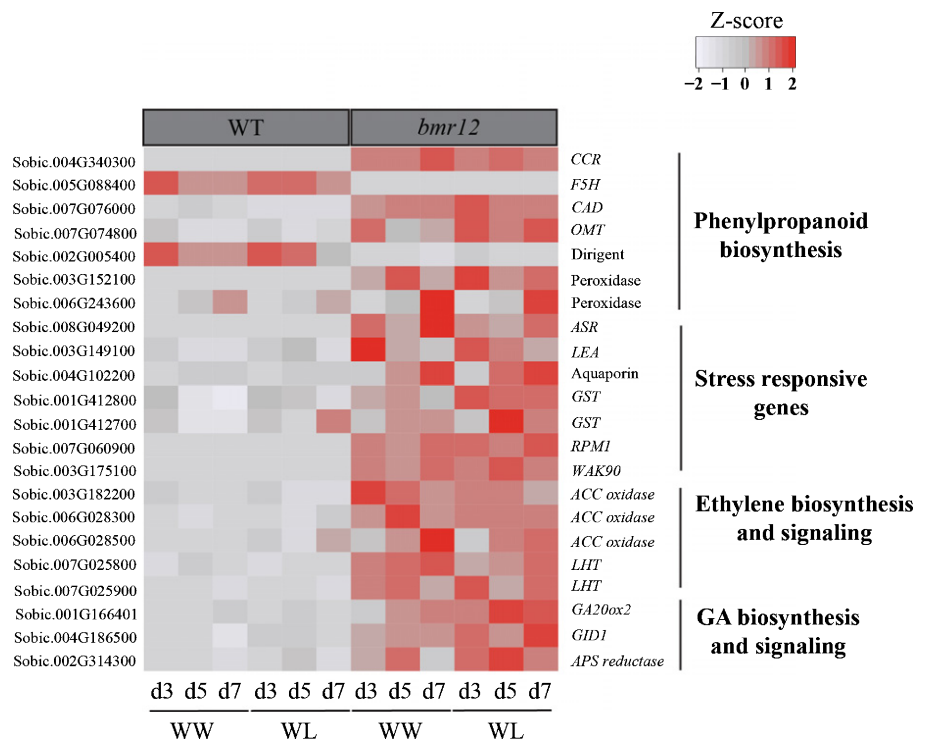
The loss of COMT impacted expression of several genes involved in lignin biosynthesis (Fig. 6). Transcript abundance of genes encoding enzymes involved in monolignol biosynthesis (a CCR, a CAD, a ferulic acid 5-hydroxylase (F5H), an *O*-methyltransferase (OMT)), and lignin polymerization (a dirigent protein and

two peroxidases) were altered in *bmr12* under both WW and WL conditions (Fig. 6). The *CCR*, *CAD* and *OMT* genes showed increased transcript abundance in *bmr12*, and genes encoding a dirigent protein and F5H exhibited decreased transcript abundance. Two genes encoding secreted peroxidases (Sobic.003G152100, ME9 and Sobic.006G243600, ME20) had higher transcript abundance in *bmr12* (Fig. 6). Sobic.003G152100 showed higher expression levels in *bmr12* at all three timepoints and Sobic.006G243600 had higher transcript levels at 5 and 7 d under both WW and WL conditions. The transcriptional responses of *bmr12* suggest that the loss of COMT altered the expression of genes related to lignin deposition.

### Loss of COMT induces stress responsive genes

Transcriptome analysis also showed increased expression of abiotic stress responsive genes in *bmr12* (Fig. 6). A gene encoding *Abscisic stress-ripening (ASR) 5* (Sobic.008G049200, ME9) homolog had higher transcript abundance in *bmr12* under both WW and WL conditions (Fig. 6). *ARS* genes respond to increased ABA levels and various abiotic stresses like drought, cold, high aluminum concentrations and salt stress (Kalifa *et al.*, 2004; Saumonneau *et al.*, 2008; Philippe *et al.*, 2010; Hu *et al.*, 2013; Li *et al.*, 2017). Higher transcript abundance of a drought associated gene (Sobic.003G149100, ME9) encoding late embryogenesis abundant (LEA) protein was observed in *bmr12* under WW and WL conditions (Fig. 6). In addition, the transcript abundance of an aquaporin gene (Sobic.004G102200, ME20) also increased in *bmr12*; its rice homolog affects arsenic tolerance (Sun *et al.*, 2018). The transcript levels of this gene

**Fig. 6** Heatmap of normalized expression values of differentially expressed genes between RTx430 (wild-type, WT) and sorghum COMT mutant, *bmr12* for 3-day-old (d3), 5-d-old (d5), and 7-d-old (d7) roots under well-watered (WW) and water-limited (WL) conditions. Normalized expression values were scaled for each gene before plotting. *CCR*, cinnamoyl-CoA reductase; *F5H*, ferulic acid 5-hydroxylase; *CAD*, cinnamyl alcohol dehydrogenase; *OMT*, *O*-methyltransferase; *ASR*, abscisic acid, stress and ripening; *LEA*, late embryogenesis abundant protein; *GST*, glutathione S-transferase; *RPM1*, RNase P mitochondrial 1; *WAK90*, wall associated kinase 90; *ACC*, 1-aminocyclopropane-1-carboxylate; *LHT*, lysine/histidine transporter; *GA20ox2*, gibberellic acid 20 oxidase 2; *GID1*, GIBBERELLIN INSENSITIVE DWARF1; *APS reductase*, adenosine-5'-phosphosulfate reductase. Color key represents the Z-score standardized values.



increased significantly at 5 and 7 days in *bmr12* under both WW and WL conditions (Fig. 6). Similarly, two genes encoding glutathione S-transferase (GST) (Sobic.001G412800, ME9 and Sobic.001G412700, ME20) were also upregulated in *bmr12*. Sobic.001G412800 showed higher levels in *bmr12* at all time-points and Sobic.001G412700 had higher transcript levels at 5 and 7 days under WW and WL conditions. Two genes associated with biotic stress, a disease resistance protein (*RPM1*, Sobic.007G060900, ME9) and a wall associated kinase (*OsWAK90*, Sobic.003G175100, ME9) also had higher transcript abundance in *bmr12*, suggesting a broader stress response.

### Loss of COMT altered genes related to hormone biosynthesis and signaling

Three genes encoding ACC oxidase (ACO; 1-aminocyclopropane-1-carboxylate oxidase), which catalyzes the conversion of 1-aminocyclopropane-1-carboxylic acid (ACC) to ethylene (Wang *et al.*, 2002), had higher transcript abundance in *bmr12* (Fig. 6). Two of these (Sobic.003G182200 and Sobic.006G028300, ME9) were elevated in *bmr12* under both WW and WL conditions, while the third gene for ACC oxidase (Sobic.006G028500) was higher only under WW condition at 7 d. In addition, two genes encoding lysine/histidine transporter 1 (LHT1) (Sobic.007G025800 and Sobic.007G025900, ME9) also had higher transcript abundance in *bmr12* under both WW and WL conditions (Fig. 6). *LHT1* encodes a plasma membrane localized ACC transporter and it is expressed in roots (with preferential expression in lateral roots) and leaf epidermis of Arabidopsis (Hirner *et al.*, 2006). These results suggest that *bmr12* roots may have higher levels of ACC, the immediate precursor of ethylene. Genetic studies in Arabidopsis and tomato have shown that ethylene and its precursor ACC inhibit lateral root formation by altering auxin distribution in roots (Ivanchenko *et al.*, 2008; Negi *et al.*, 2010; Lewis *et al.*, 2011). Therefore, it is possible that higher levels of ethylene could be a factor in reducing LRD in *bmr12* mutants. To address this hypothesis, we examined the effect of exogenous ACC application (50, 100, 200, 500 and 1 mM) on wild-type and *bmr12* roots (Fig. S6). We did not observe any effect on LRD at 50, 100 and 200  $\mu$ M concentration. Further increasing ACC concentration (500 and 1 mM) resulted in inhibition of primary root growth of both genotypes. Thus, higher ethylene levels are unlikely to be associated with the LRD phenotype of *bmr12* mutants.

We also found that genes related to GA biosynthesis (*GA20-oxidase 2*, *GA20ox2*) and GA signaling (gibberellin receptor: *GIBBERELLIN-INSENSITIVE DWARF1 LIKE 2*, *GID1L2*) have higher transcript abundance in *bmr12* (Fig. 6). Under WW conditions, the expression of *GA20ox2* (Sobic.001G166401, ME9) was significantly upregulated in *bmr12* at 5 and 7 d relative to wild-type. Under WL conditions, transcript accumulation of *GA20ox2* was significantly higher in *bmr12* at all three time points relative to wild-type. GA20-oxidases are the final rate limiting enzymes in GA biosynthesis and changes in expression of *GA20ox2* can regulate GA levels (Huang *et al.*, 1998; Ashikari *et al.*, 2002). Expression level of *GID1L2* (Sobic.004G186500;

ME9) was also upregulated in *bmr12* under WW and WL conditions. Transcript abundance of an adenosine-5'-phosphosulfate (APS) reductase (Sobic.002G314300; ME9) gene was also significantly increased in *bmr12* roots under both conditions; its Arabidopsis homolog is induced in response to GA (Koprivova *et al.*, 2008). These results suggest that GA metabolism and signaling are altered in *bmr12*.

### Role of GA in reducing lateral root density in *bmr12*

GA has been reported as a negative regulator of lateral root growth in Arabidopsis (Lv *et al.*, 2018) and *Populus* species (Guo *et al.*, 2010), hence GA may mediate the reduced LRD observed in *bmr12*. To examine this possibility, wild-type and *bmr12* seedlings were treated with exogenous GA<sub>3</sub> at 1, 10 and 100  $\mu$ M concentrations for 6 d under WW condition under WW conditions (Fig. 7). The GA application had a significant effect on SL, LRD and RSL ratio in both genotypes, but did not alter RL. Although both wild-type and *bmr12* showed increase in SL and decrease in RSL ratio with increasing dosage of GA<sub>3</sub>, a greater increase in SL and reduction in RSL was observed in *bmr12* than wild-type (Fig. 7). LRD in *bmr12* seedlings was also more sensitive to GA application than wild-type. While treatment with 1 and 10  $\mu$ M GA resulted in significant reduction in LRD in *bmr12*; LRD in the wild-type was not altered at 1  $\mu$ M concentration and significant reduction was observed starting with 10  $\mu$ M GA concentration. Further increase in GA dosage to 100  $\mu$ M also reduced LRD in the wild-type. In contrast, *bmr12* showed significant increase in LRD with 100  $\mu$ M GA concentration. We next treated both genotypes with a GA inhibitor, DMZ. DMZ treatment reduced LRD in the wild-type but had no effect on *bmr12* roots. DMZ had no effect on primary RL of both genotypes (Fig. S7). Taken together, these results showed that *bmr12* has increased sensitivity to GA application at low concentrations and is insensitive to the GA inhibitor relative to wild-type seedlings.

### Discussion

Given the importance of lignin in maintaining cell wall integrity and xylem function for transporting water, we examined how altered lignin composition and deposition affects root growth and response to water stress using *bmr12*. To this end, we examined the physiological and transcriptional consequences of the null mutant *bmr12-ref* on sorghum root growth and in response to water stress. *Bmr12* encodes the enzyme COMT, which catalyzes the penultimate step in monolignol biosynthesis. At the seedling stage, root morphological alterations were observed in *bmr12* which include reduced LRD (Fig. 1c) and LRP initiation (Fig. 1e). In addition to LRP, anatomy of *bmr12* roots is also altered with increased total root, cortex and stele cross-sectional areas under WW conditions, which result in a thicker primary root system in *bmr12* relative to the wild-type (Fig. 2). Analysis of post-flowering roots indicate that *bmr12* has reduced nodal root angle at maturity under both irrigated and nonirrigated field conditions (Fig. 3). Therefore, reduced LRD in embryonic roots and reduced angular spread of post-embryonic nodal roots

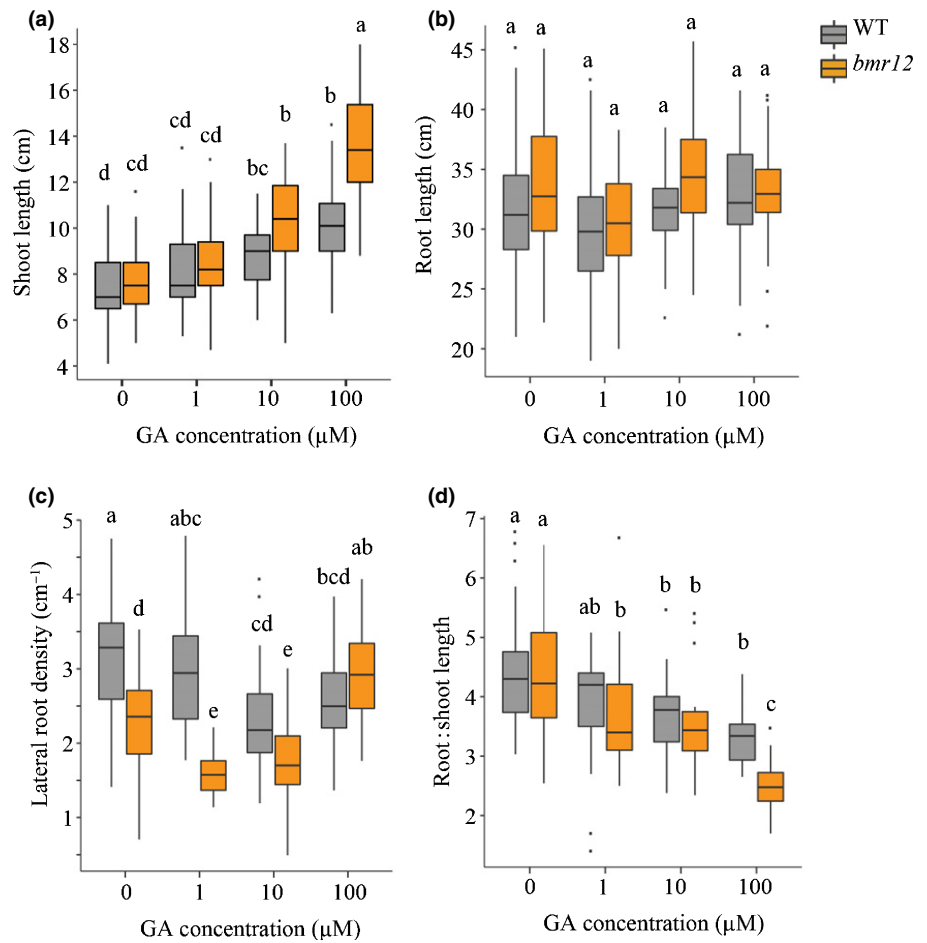


**Fig. 7** Role of gibberellic acid (GA) in reducing lateral root density in sorghum. Effect of exogenous GA application on (a) shoot length, (b) root length, (c) lateral root density, and (d) root to shoot length ratio in RTx430 (wild-type, WT) and sorghum COMT mutant, *bmr12* under well-watered conditions. GA concentrations of 1, 10 and 100 μM were applied ( $n = 30$ ). The black lines within the boxes marks the median, the upper and lower whiskers represent the first and third quartile of the data, respectively. Outliers are shown as black dots and signify values smaller/greater than first/third quartile, multiplied by 1.5, respectively. For statistical analysis, Tukey's test was performed, and different letters indicate significantly different means at  $P < 0.05$ .

suggest that loss of COMT specifically impacts LRD. The absence of a lateral root phenotype in *bmr6* (Table S1) which is another mutant with reduced lignin levels, suggests that reduced LRD is not associated with reduced lignin concentration in *bmr12*. Reduced LRD in maize *COMT* mutant, *bm3* (Fig. S1) further suggests that reduction in LRD with loss of COMT activity is not limited to sorghum. Furthermore, overexpression of the turfgrass *Carex rigescens* *COMT* in Arabidopsis was associated with increased lateral root number (Zhang *et al.*, 2019). This result supports our findings that COMT activity alters LRD in sorghum and maize. Most common physiological responses to drought stress in plants involve strategic reduction and relocation of metabolic energy towards the tissues/organs which help to mitigate the stress and enhance water uptake and reduce biomass loss. In this context, one strategy under WL conditions could be to promote vertical root growth for exploring deeper soil strata for water (Fang *et al.*, 2017). Narrower root angle can enhance rooting depth and a thicker root system can provide mechanical support in dry soils (Mace *et al.*, 2012; Joshi *et al.*, 2017). In this context, our findings that some of the wild-type root responses to WL conditions were evident in *bmr12* even under WW conditions suggest a possible role for lignin deposition as one of the means for drought adaptation.

Visible and fluorescence imaging are highly sensitive tools for capturing dynamic stress responses in a nondestructive manner

and have been successfully used for early detection of drought stress in Arabidopsis, barley and maize (Lazar *et al.*, 2006; De Sousa *et al.*, 2017; Yao *et al.*, 2018). In the present study, temporal growth analysis through RGB imaging indicated that temporal biomass accumulation of *bmr12* is similar to water-stressed wild-type even when *bmr12* is well-watered (Fig. 4a). However, *bmr12* maintained growth under WL conditions for a longer time than wild-type. This difference cannot be simply explained by lower water use by smaller *bmr12* plants as the water use under water stress conditions is similar for both genotypes for most days of the experiment (Table S2). Further, water levels were adjusted regularly thus mitigating any prolonged advantage due to reduced water use by *bmr12* plants under water stress. Further, transpiration rates for a unit leaf area were similar for both genotypes thus excluding any inherent difference in gas exchange due to, for instance, altered stomatal density. Collectively, these data suggest that *bmr12* plants are more resistant to water stress. Our fluorescence clustering analysis provided insights into the overall whole plant response, where *bmr12* plants under WW conditions have fluorescence signatures similar to the wild-type plants under WL conditions (Fig. 5). We also identified two specific cc (8–9) that were specific to WL in the later stages of treatment. In addition, gas exchange parameters suggested that *bmr12* might also show earlier reduction in gas exchange than wild-type (Fig. S4). Collectively, our root and temporal shoot growth response results

suggest that loss of COMT in *bmr12* result in altered shoot growth similar to a stressed wild-type even in the absence of water stress as a consequence of changes in monolignol biosynthesis.

Seedling root transcriptome analyses brought forth three key features regarding the loss of COMT: first, it altered expression of additional genes involved in phenylpropanoid metabolism that is indicative of altered lignin deposition; second, it increased stress responsive gene expression in the absence of stress stimuli suggesting a role for COMT in biotic and abiotic stress responses and third, it led to altered GA and ethylene biosynthesis and signaling gene expression that may affect lateral root growth. Loss of COMT results in accumulation of 5-hydroxyconiferyl groups, an intermediate in monolignol metabolism (Palmer *et al.*, 2010; Sattler *et al.*, 2012). Elevated levels of this compound interfere with pollen development, causing male sterility (Weng *et al.*, 2010; Tetreault *et al.*, 2020). Therefore, overaccumulation of intermediate compounds such as 5-hydroxyconiferyl groups from monolignol metabolism can have negative impacts on plant growth and development. The decreased transcript abundance of *F5H* and increased expression of *CCR* and *CAD* suggests a molecular mechanism whereby, in COMT deficient plants, decreased *F5H* expression likely reduced accumulation of 5-hydroxyconiferyl groups and increased substrates for CCR and CAD, potentially leading to their greater transcript abundance. Furthermore, Mäule staining was used to visualize differences in S-lignin deposition in wild-type and *bmr12* cell walls (Fig. 1a). Wild-type has increased staining under WL conditions and *bmr12* stained less than the wild-type in both WW and WL conditions (Fig. 1a). In the transcriptome analysis, increased expression of *F5H* was observed in the wild-type under WL conditions (Fig. 6) which positively correlates with increased Mäule staining in the wild-type under WL conditions. However, *bmr12* displayed reduced transcript abundance of *F5H* as compared to the wild-type in both WW and WL conditions (Fig. 6). In addition, *bmr12* also had higher transcript levels of two genes encoding secreted peroxidases (Fig. 6), which may be involved in lignin polymerization. Previously, COMT mutant in Arabidopsis had decreased expression of several phenylpropanoid pathway related genes (Vanholme *et al.*, 2012). However, we did not observe downregulation of phenylpropanoid pathway genes in *bmr12* seedlings. Only transcript abundance of *F5H* was reduced, which is consistent with its specific role, together with COMT, in the synthesis of sinapyl alcohol.

Previous studies have shown the involvement of COMT in stress tolerance (Vincent *et al.*, 2005; Li *et al.*, 2010; Yang *et al.*, 2019). We found *bmr12* to have increased transcript abundance of a stress responsive gene, *ASR5* and a drought induced LEA protein (Fig. 6). GST genes were also upregulated in *bmr12* which may help to alleviate oxidative stress by actively scavenging reactive oxygen species during biotic and abiotic stress (Roxas *et al.*, 1997; Roxas *et al.*, 2000; Jiang *et al.*, 2010). Two genes that are known to be induced in response to both biotic and abiotic stresses, *RPM1* and *WAK90*, had higher transcript levels in *bmr12* relative to the wild-type in both WW and WL conditions. Downregulation of lignin biosynthetic genes has been reported to induce latent defense response in the absence of biotic and abiotic stress in Arabidopsis (Gallego-

Giraldo *et al.*, 2011; Zhao & Dixon, 2014; Gallego-Giraldo *et al.*, 2020). This study also highlights the interconnection between COMT activity and stress responses as its loss results in increased expression of several stress responsive genes.

Transcript levels of *GA20ox2*, a key GA biosynthesis gene, were increased in *bmr12* under WW and WL conditions with no alterations in expression of GA catabolic genes (Table S5), which likely resulted in higher GA levels. GA induces the stress responsive gene *ASR5* in other systems, and ASR5 protein functions downstream of *GID1* and *SLENDER RICE1* (*SLR1*) in GA signaling (Koprivova *et al.*, 2008; Takasaki *et al.*, 2008). Evidence indicates that GA is a negative regulator of lateral root growth in several plant species (Fu & Harberd, 2003; Guo *et al.*, 2010; Lv *et al.*, 2018; Mignolli *et al.*, 2019). The greater sensitivity of *bmr12* to lower dosage of exogenous GA that we observed suggests that GA is associated with reduced lateral root phenotype. However, at 100  $\mu$ M GA *bmr12* and wild-type showed different responses, reducing and increasing LRD in wild-type and *bmr12*, respectively (Fig. 7). The increase in LRD in *bmr12* could be a consequence of faster initiation of GA feedback regulation to maintain the optimal concentration of GA required for normal root growth which is not evident in wild-type plants due to lower baseline GA levels. Increasing GA dosage had no effect on RL in either genotype, which indicates that GA application at these specified dosages specifically impacts seedling LRD but not RL. GA inhibitor, DMZ had no effect on LRD in *bmr12*, but significantly reduced LRD in the wild-type (Fig. S7). DMZ application may decrease GA to levels insufficient for supporting normal root growth in the wild-type. Differential sensitivity was observed between wild-type and *bmr12* with GA and DMZ applications, suggesting that GA is involved in reducing LRD in *bmr12*. Previous studies in Arabidopsis (Lv *et al.*, 2018) and poplar (Guo *et al.*, 2010) have shown crosstalk between GA and auxin during lateral root formation (Fu & Harberd, 2003). Although the differential regulation of genes related to auxin biosynthesis and its signaling between wild-type and *bmr12* were not observed in this study, the localized spatial-temporal auxin maxima required for lateral root emergence may have been below the resolution of detection using RNAseq on whole roots. Although transcript levels of ACO were increased in *bmr12* relative to the wild-type we found no direct evidence that ethylene had a role in LRD reduction. Rather, it may be involved in regulating other aspects of root development in relation to stress in *bmr12*. Some studies have suggested a role for both ethylene and GA in regulating cell proliferation during osmotic stress (Skirycz *et al.*, 2010; Skirycz *et al.*, 2011). Ethylene has been shown to inhibit root growth in Arabidopsis and tomato via auxin-ethylene crosstalk and inhibition of cell proliferation in root meristem (Negi *et al.*, 2008; Negi *et al.*, 2010; Street *et al.*, 2015). However, its role in *bmr12* needs further investigation.

The involvement of GA biosynthesis and signaling in root growth under water limitation is not well-understood. In Arabidopsis, water limitation was shown to reduce GA levels (Colebrook *et al.*, 2014), while opposite effects were observed in roots of wild emmer accession of wheat, where drought tolerant genotypes showed decreased *GA20ox* expression that led to elevated GA

levels to maintain the growth of primary root meristem (Krugman *et al.*, 2011). GA and auxin have been shown to alter the ratio of S : G units during lignin synthesis (Aloni *et al.*, 1990) indicating responsiveness of monolignol biosynthesis to phytohormones. Changes in the expression of monolignol pathway genes has been observed in response to biotic and abiotic stresses (Cesarino, 2019), and perturbations in lignin synthesis can also induce expression of stress related pathway genes in *Arabidopsis* (Vanholme *et al.*, 2012). In the present study, we observed that loss of COMT activity induced the expression of genes related to stress, GA, ethylene and phenylpropanoid pathway. Although pharmacological analysis of GA and ACC suggested a role of GA in reduced LRD in *bmr12*, our observations cannot exclude contributions from additional mechanisms. In summary, this work highlights the role of COMT in regulating LRD and stress responses. Future research will focus on the molecular basis of this role in stress adaptation in spatial and temporal context.

## Acknowledgements

The authors thank John Toy, Tammy Gries and Pat O'Neill for their technical assistance, Prof. Paul Staswick for valuable input during research and writing of this manuscript, Drs Heather Van Buskirk and Puneet Paul for critically reviewing this manuscript, and Drs James Eudy and Alok Dhar for sequencing assistance. Illumina HiSeq 2500 sequencing was performed at the University of Nebraska Medical Center Genomics Core Facility, Omaha, NE, USA. This research was supported by the US Department of Agriculture, Agricultural Research Service (USDA-ARS) CRIS project 3042-21220-033-00D. The USDA-ARS is an equal opportunity affirmative action employer and all agency services are available without discrimination. The mention of commercial products and organizations in this article is solely to provide specific information. It does not constitute endorsement by USDA-ARS over other products and organizations not mentioned.

## Author contributions

SES, HW and MS designed the research, MS performed all the experiments and analyzed results, FZ and HY performed image processing, MS, SES and HW wrote the manuscript, and all authors reviewed the manuscript.

## ORCID

Manny Saluja  <https://orcid.org/0000-0002-9267-0882>  
 Scott E. Sattler  <https://orcid.org/0000-0002-6814-4073>  
 Harkamal Walia  <https://orcid.org/0000-0002-9712-5824>  
 Hongfeng Yu  <https://orcid.org/0000-0002-0596-8227>  
 Feiyu Zhu  <https://orcid.org/0000-0001-6863-7137>

## References

- Abramoff MD, Magalhaes PJ, Ram SJ. 2004. Image processing with ImageJ. *Biophotonics International* 11: 36–42.
- Ali F, Scott P, Bakht J, Chen Y, Lubberstedt T. 2010. Identification of novel *brown midrib* genes in maize by tests of allelism. *Plant Breeding* 129: 724–726.
- Aloni R, Tollier MT, Monties B. 1990. The role of auxin and gibberellin in controlling lignin formation in primary phloem fibers and in xylem of *Coleus blumei* stems. *Plant Physiology* 94: 1743–1747.
- Ashikari M, Sasaki A, Uegucghi-Tanaka M, Itoh H, Nishimura A, Datta S, Ishiyama K, Saito T, Kobayashi M, Khush GS *et al.* 2002. Loss-of-function of a rice gibberellin biosynthetic gene, *GA20 oxidase (GA20ox-2)*, led to the rice 'green revolution'. *Breeding Science* 52: 143–150.
- Baucher M, Bernard-Vailhe MA, Chabbert B, Besle JM, Opsomer C, Montagu MV, Botterman J. 1999. Down-regulation of cinnamyl alcohol dehydrogenase in transgenic alfalfa (*Medicago sativa* L.) and the effect on lignin composition and digestibility. *Plant Molecular Biology* 39: 437–447.
- Baucher M, Chabbert B, Pilate G, Van Doorselaere J, Tollier MT, Petit-Conil M, Cornu D, Monties B, Van Montagu M, Inze D *et al.* 1996. Red xylem and higher lignin extractability by down-regulating a cinnamyl alcohol dehydrogenase in poplar. *Plant Physiology* 112: 1479–1490.
- Berger B, Parent B, Tester M. 2010. High-throughput shoot imaging to study drought responses. *Journal of Experimental Botany* 61: 3519–3528.
- Bout S, Vermerris W. 2003. A candidate-gene approach to clone the sorghum *Brown midrib* gene encoding caffeic acid O-methyltransferase. *Molecular Genetics and Genomics* 269: 205–214.
- Cabane M, Affif D, Hawkins S. 2012. Lignins and abiotic stresses. In: Jouanin L, Lapiere C, eds. *Advances in botanical research*. Cambridge, MA, USA: Academic Press, 219–262.
- Cambell MT, Knecht AC, Berger B, Brien CJ, Wang D, Walia H. 2015. Interating image-based phenomics and association analysis to dissect the genetic architecture of temporal salinity response in rice. *Plant Physiology* 168: 1476–1489.
- Cesarino I. 2019. Structural features and regulation of lignin deposited upon biotic and abiotic stresses. *Current Opinion in Biotechnology* 56: 209–214.
- Chabannes M, Barakate A, Catherine L, Jane MM, Ralph J, Pean M, Danoun S, Halpin C, Pettenati JG, Boudet AM. 2001. Strong decrease in lignin content without significant alteration of plant development is induced by simultaneous down-regulation of cinnamoyl CoA reductase (CCR) and cinnamyl alcohol dehydrogenase (CAD) in tobacco plants. *The Plant Journal* 28: 257–270.
- Chen F, Dixon RA. 2007. Lignin modification improves fermentable sugar yields for biofuel production. *Nature Biotechnology* 25: 759–761.
- Choat B, Nolf M, Lopez R, Peter JMR, Carins-Murphy MR, Creek D, Brodrribb TJ. 2019. Non-invasive imaging shows no evidence of embolism repair after drought in tree species of two genera. *Tree Physiology* 39: 113–121.
- Colebrook EH, Thomas SG, Phillips AL, Hedden P. 2014. The role of gibberellin signalling in plant responses to abiotic stress. *Journal of Experimental Biology* 217: 67–75.
- Cook CM, Daudi A, Millar DJ, Bindschedler LV, Khan S, Bolwell GP, Devoto A. 2012. Transcriptional changes related to secondary wall formation in xylem of transgenic lines of tobacco altered for lignin or xylan content which show improved saccharification. *Phytochemistry* 74: 79–89.
- Dante PF, Campbell MT, Folsom JJ, Cui X, Kruger GR, Baenziger PS, Walia H. 2013. Introgression of novel traits from a wild wheat relative improves drought adaptation in wheat. *Plant Physiology* 161: 1806–1819.
- De Sousa CA, de Paiva DS, Casari RADCN, de Oliveira NG, Molinari HBC, Kobayashi AK, Magalhaes PC, Gomide RL, Souza MT Jr. 2017. A procedure for maize genotypes discrimination to drought by chlorophyll fluorescence imaging rapid light curves. *Plant Methods* 13: 61.
- Dien BS, Sarath G, Pedersen JF, Sattler SE, Chen H, Funnell-Harris DL, Nichols NN, Cotta MA. 2009. Improved sugar conversion and ethanol yield for forage sorghum (*Sorghum bicolor* L. Moench) lines with reduced lignin contents. *BioEnergy Research* 2: 153–164.
- Fan L, Linker R, Gepstein S, Tanimoto E, Yamamoto R, Neumann PM. 2006. Progressive inhibition by water deficit of cell wall extensibility and growth along the elongation zone of maize roots is related to increased lignin metabolism and progressive stelar accumulation of wall phenolics. *Plant Physiology* 140: 603–612.
- Fang Y, Du Y, Wang J, Wu A, Qiao S, Xu B, Zhang A, Siddique KHM, Chen Y. 2017. Moderate drought stress affected root growth and grain yield in old,

- modern and newly released cultivars of winter wheat. *Frontiers in Plant Science* 8: 672.
- Franke R, Humphreys JM, Hemm MR, Denault JW, Ruegger MO, Cusumano JC, Chapple C. 2002. The Arabidopsis REF8 gene encodes the 3-hydroxylase of phenylpropanoid metabolism. *The Plant Journal* 30: 33–45.
- Fu C, Mielenz JR, Xiao X, Ge Y, Hamilton CY, Rodriguez M, Chen F, Foston M, Ragauskas A, Bouton J *et al.* 2011. Genetic manipulation of lignin reduces recalcitrance and improves ethanol production from switchgrass. *Proceedings of the National Academy of Science, USA* 108: 3803–3808.
- Fu X, Harberd NP. 2003. Auxin promotes Arabidopsis root growth by modulating gibberellin response. *Nature* 421: 740–743.
- Furtado A, Lupoi JS, Hoang NV, Healey A, Singh A, Simmons BA, Robert JH. 2014. Modifying plants for biofuel and biomaterial production. *Plant Biotechnology Journal* 12: 1246–1258.
- Gallego-Giraldo L, Jikumaru Y, Kamiya Y, Tang Y, Dixon RA. 2011. Selective lignin downregulation leads to constitutive defense response expression in alfalfa (*Medicago sativa* L.). *New Phytologist* 190: 627–639.
- Gallego-Giraldo L, Liu C, Pose-Albacete S, Pattathil S, Peralta AG, Young J, Westpheling J, Hahn MG, Rao X, Knox JP *et al.* 2020. ARABIDOPSIS DEHISCENCE ZONE POLYGALACTURONASE 1 (ADPG1) releases latent defense signals in stems with reduced lignin content. *Proceedings of the National Academy of Sciences, USA* 117: 3281–3290.
- Guo J, Strauss SH, Tsai CJ, Fang K, Chen Y, Jiang X, Busov VB. 2010. Gibberellins regulate lateral root formation in *Populus* through interactions with auxin and other hormones. *The Plant Cell* 22: 623–639.
- Harb A, Krishnan A, Ambavaram MMR, Pereira A. 2010. Molecular and physiological analysis of drought stress in Arabidopsis reveals early responses leading to acclimation in plant growth. *Plant Physiology* 154: 1254–1271.
- Hirner A, Ladwig F, Stransky H, Okumoto S, Keinath M, Harms A, Frommer WB, Kocha W. 2006. Arabidopsis LHT1 is a high-affinity transporter for cellular amino acid uptake in both root epidermis and leaf mesophyll. *The Plant Cell* 18: 1931–1946.
- Hu W, Huang C, Deng X, Zhou S, Chen L, Li Y, Wang C, Ma C, Yuan Q, Wang Y *et al.* 2013. *TaASR1*, a transcription factor gene in wheat, confers drought stress tolerance in transgenic tobacco. *Plant, Cell & Environment* 36: 1449–1464.
- Huang J, Gu M, Lai Z, Fan B, Shi K, Zhou YH, Yu JQ, Chen Z. 2010. Functional analysis of the Arabidopsis *PAL* gene family in plant growth, development and response to environmental stress. *Plant Physiology* 153: 1526–1538.
- Huang S, Raman AS, Ream JE, Fujiwara H, Cerny RE, Brown SM. 1998. Overexpression of 20-oxidase confers a gibberellin-overproduction phenotype in Arabidopsis. *Plant Physiology* 118: 773–781.
- Ivanchenko MG, Muday GK, Dubrovsky JG. 2008. Ethylene–auxin interactions regulate lateral root initiation and emergence in *Arabidopsis thaliana*. *The Plant Journal* 55: 335–347.
- Jiang HW, Liu MJ, Chen IC, Huang CH, Chao LY, Hsieh HL. 2010. A glutathione S-transferase regulated by light and hormones participates in the modulation of Arabidopsis seedling development. *Plant Physiology* 154: 1646–1658.
- Jones L, Ennos AR, Turner SR. 2001. Cloning and characterization of *irregular xylem4* (*irx4*): a severely lignin-deficient mutant of Arabidopsis. *The Plant Journal* 26: 205–216.
- Joshi DC, Singh V, Hunt C, Mace E, Van Oosterom E, Sulman R, Jordan D, Hammer G. 2017. Development of a phenotyping platform for high throughput screening of nodal root angle in sorghum. *Plant Methods* 13: 56.
- Kalifa Y, Perlson E, Gilad A, Konrad Z, Scolnik PA, Bar-Zvi D. 2004. Overexpression of the water and salt stress-regulated *Asr1* gene confers an increased salt tolerance. *Plant, Cell & Environment* 27: 1459–1468.
- Kavousi B, Daudi A, Cook CM, Joseleau JP, Ruel K, Devoto A, Bolwell GP, Blee KA. 2010. Consequences of antisense down-regulation of a lignification-specific peroxidase on leaf and vascular tissue in tobacco lines demonstrating enhanced enzymic saccharification. *Phytochemistry* 71: 531–542.
- Khanna R, Schmid L, Walter A, Nieto J, Siegwart R, Liebisch F. 2019. A spatial temporal spectral framework for plant stress phenotyping. *Plant Methods* 15: 13.
- Koprivova A, North KA, Kopriva S. 2008. Complex signaling network in regulation of adenosine 5'-phosphosulfate reductase by salt stress in Arabidopsis roots. *Plant Physiology* 146: 1408–1420.
- Krugman T, Peleg Z, Quansah L, Chagué V, Korol AB, Nevo E, Saranga Y, Fait A, Chalhouh B, Fahima T. 2011. Alteration in expression of hormone-related genes in wild emmer wheat roots associated with drought adaptation mechanisms. *Functional & Integrative Genomics* 11: 565–583.
- Kyriakopoulos G, Kolovos K, Chalikias M. 2010. Environmental sustainability and financial feasibility evaluation of woodfuel biomass used for a potential replacement of conventional space heating sources. Part II: a combined Greek and the nearby Balkan countries case study. *Operations Research* 10: 57–69.
- Langfelder P, Horvath S. 2008. WGCNA: an R package for weighted correlation analysis. *BMC Bioinformatics* 9: 559.
- Lazar D, Susila P, Naus J. 2006. Early detection of plant stress from changes in distributions of chlorophyll a fluorescence parameters measured with fluorescence imaging. *Journal of Fluorescence* 16: 173–176.
- Lewis DR, Negi S, Sukumar P, Muday GK. 2011. Ethylene inhibits lateral root development, increases IAA transport and expression of PIN3 and PIN7 auxin efflux carriers. *Development* 138: 3485–3495.
- Li J, Li Y, Yin J, Jiang J, Zhang M, Guo X, Ye Z, Zhao Y, Xiong H, Zhang Z *et al.* 2017. *OsASR5* enhances drought tolerance through stomatal closure pathway associated with ABA and H<sub>2</sub>O<sub>2</sub> signalling in rice. *Plant Biotechnology Journal* 15: 183–196.
- Li XJ, Yang MF, Chen H, Qu LQ, Chen F, Shen SH. 2010. Abscisic acid pretreatment enhances salt tolerance of rice seedlings: proteomic evidence. *Biochimica et Biophysica Acta* 1804: 929–940.
- Love MI, Huber W, Anders S. 2014. Moderated estimation of fold change and dispersion for RNA-seq data with DESeq2. *Genome Biology* 15: 550.
- Lv S, Yu D, Sun Q, Jiang J. 2018. Activation of gibberellin 20-oxidase 2 undermines auxin-dependent root and root hair growth in NaCl-stressed Arabidopsis seedlings. *Plant Growth Regulation* 84: 225–236.
- Mace E, Singh V, Van Oosterom E, Hammer G, Hunt C, Jordan D. 2012. QTL for nodal root angle in sorghum (*Sorghum bicolor* L. Moench) co-locate with QTL for traits associated with drought adaptation. *Theoretical and Applied Science* 124: 97–109.
- Mignolli F, Vidoz ML, Picciarelli P, Mariotti L. 2019. Gibberellins modulate auxin responses during tomato (*Solanum lycopersicum* L.) fruit development. *Physiologia Plantarum* 165: 768–779.
- Mir RR, Zaman-Allah M, Sreenivasulu N, Trethowan R, Varshney RK. 2012. Integrated genomics, physiology and breeding approaches for improving drought tolerance in crops. *Theoretical and Applied Genetics* 125: 625–645.
- Negi S, Ivanchenko MG, Muday GK. 2008. Ethylene regulates lateral root formation and auxin transport in *Arabidopsis thaliana*. *The Plant Journal* 55: 175–187.
- Negi S, Sukumar P, Liu X, Cohen JD, Muday GK. 2010. Genetic dissection of the role of ethylene in regulating auxin-dependent lateral and adventitious root formation in tomato. *The Plant Journal* 61: 3–15.
- Palmer NA, Sattler SE, Saathoff AJ, Funnell D, Pedersen JF, Sarath G. 2008. Genetic background impacts soluble and cell wall-bound aromatics in *brown midrib* mutants of sorghum. *Planta* 229: 115–127.
- Palmer NA, Sattler SE, Saathoff AJ, Sarath G. 2010. A continuous, quantitative fluorescent assay for plant caffeic acid O-methyltransferases. *Journal of Agricultural and Food Chemistry* 58: 5220–5226.
- Pedersen JF, Funnell DL, Toy JJ, Oliver AL, Grant RJ. 2006. Registration of twelve grain sorghum genetic stocks near-isogenic for the brown midrib genes *bmr-6* and *bmr-12*. *Crop Science* 46: 491–492.
- Philippe R, Courtois B, McNally KL, Mournet P, El-Malki R, Le Paslier MC, Fabre D, Billot C, Brunel D, Glaszmann JC *et al.* 2010. Structure, allelic diversity and selection of *Asr* genes, candidate for drought tolerance, in *Oryza sativa* L. and wild relatives. *Theoretical and Applied Genetics* 121: 769–787.
- Pincon G, Maury S, Hoffmann L, Geoffroy P, Lapierre C, Pollet B, Legrand M. 2001. Repression of O-methyltransferase genes in transgenic tobacco affects lignin synthesis and plant growth. *Phytochemistry* 57: 1167–1176.
- Roxas VP, Lodhi SA, Garrett DK, Mahan JR, Allen RD. 2000. Stress tolerance in transgenic tobacco seedlings that overexpress glutathione S-transferase/glutathione peroxidase. *Plant and Cell Physiology* 41: 1229–1234.

- Roxas VP, Smith RK Jr, Allen ER, Allen RD. 1997. Overexpression of glutathione S-transferase/glutathione peroxidase enhances the growth of transgenic tobacco seedlings during stress. *Nature Biotechnology* 15: 988–991.
- Sattler SE, Funnell-Harris DL, Pedersen JF. 2010. Efficacy of singular and stacked *brown midrib 6* and *12* in the modification of lignocellulose and grain chemistry. *Journal of Agricultural and Food Chemistry* 58: 3611–3616.
- Sattler SE, Palmer NA, Saballos A, Greene AM, Xin Z, Sarath G, Vermerris W, Pedersen JF. 2012. Identification and characterization of four missense mutations in *Brown midrib 12* (*Bmr12*), the caffeic O-methyltransferase (COMT) of sorghum. *Bioenergy Research* 5: 855–865.
- Sattler SE, Saathoff AJ, Haas EJ, Palmer NA, Funnell-Harris DL, Sarath G, Pedersen JF. 2009. A nonsense mutation in a cinnamyl alcohol dehydrogenase gene is responsible for the sorghum *brown midrib6* phenotype. *Plant Physiology* 150: 584–595.
- Saumonneau A, Agasse A, Bidoyen MT, Lallemand M, Cantereau A, Medici A, Laloi M, Atanassova R. 2008. Interaction of grape ASR proteins with DREB transcription factor in the nucleus. *FEBS Letters* 582: 3281–3287.
- Scully ED, Gries T, Funnell-Harris DL, Xin Z, Kovacs FA, Vermerris W, Sattler SE. 2016. Characterization of novel *Brown midrib 6* mutations affecting lignin biosynthesis in sorghum. *Journal of Integrative Plant Biology* 58: 136–149.
- Skirycz A, Claeys H, De Bodt S, Oikawa A, Shinoda S, Andriankaja M, Maleux K, Eloy NB, Coppens F, Yoo SD *et al.* 2011. Pause-and-stop: the effects of osmotic stress on cell proliferation during early leaf development in Arabidopsis and a role for ethylene signaling in cell cycle arrest. *The Plant Cell* 23: 1876–1888.
- Skirycz A, De Bodt S, Obata T, De Clercq I, Claeys H, De Rycke R, Andriankaja M, Van Aken O, Van Breusegem F, Fernie AR *et al.* 2010. Developmental stage specificity and the role of mitochondrial metabolism in the response of Arabidopsis leaves to prolonged mild osmotic stress. *Plant physiology* 152: 226–244.
- Street IH, Aman S, Zubo Y, Ramzan A, Wang X, Shakeel SN, Kieber JJ, Schaller GE. 2015. Ethylene inhibits cell proliferation of the Arabidopsis root meristem. *Plant physiology* 169: 338–350.
- Sun SK, Chen Y, Che J, Konishi N, Tang Z, Miller AJ, Ma JF, Zhao FJ. 2018. Decreasing arsenic accumulation in rice by overexpressing *OsNIP1;1* and *OsNIP3;3* through disrupting arsenite radial transport in roots. *New Phytologist* 219: 614–653.
- Takasaki H, Mahmood T, Matsuoka M, Matsumoto H, Komatsu S. 2008. Identification and characterization of gibberellin-regulated protein, which is ARS5, in the basal region of rice leaf sheaths. *Molecular Genetics and Genomics* 279: 359–370.
- Tetreault HM, Gries T, Palmer NA, Funnell-Harris DL, Sato S, Ge Z, Sarath G, Sattler SE. 2020. Overexpression of ferulate 5-hydroxylase increases syringyl units in *Sorghum bicolor*. *Plant Molecular Biology* 103: 269–285.
- Tu Y, Rochfort S, Liu Z, Ran Y, Griffith M, Badendorst P, Louie GV, Bowman ME, Smith KF, Noel JP *et al.* 2010. Functional analysis of caffeic acid O-methyltransferase and cinnamoyl-CoA-reductase genes from perennial ryegrass (*Lolium perenne*). *The Plant Cell* 22: 3357–3373.
- Vanholme R, Cesarino I, Rataj K, Xiao Y, Sundin L, Goeminne G, Kim H, Cross J, Morreel K, Araujo P *et al.* 2013. Caffeoyl Shikimate Esterase (CSE) is an enzyme in the lignin biosynthetic pathway in Arabidopsis. *Science* 341: 1103–1106.
- Vanholme R, Storme V, Vanholme B, Sundin L, Christensen JH, Goeminne G, Halpin C, Rohde A, Morreel K, Boerjan W. 2012. A systems biology view of responses to lignin biosynthesis perturbations in Arabidopsis. *The Plant Cell* 24: 3506–3529.
- Vignols F, Rigau J, Torres MA, Capellades M, Puigdomenech P. 1995. The *brown midrib3* (*bm3*) mutation in maize occurs in the gene encoding caffeic acid O methyltransferase. *The Plant Cell* 7: 407–416.
- Vincent D, Lapierre C, Pollet B, Cornic G, Negroni L, Zivy M. 2005. Water deficits affect caffeate O-methyltransferase, lignification, and related enzymes in maize leaves. A proteomic investigation. *Plant Physiology* 137: 949–960.
- Vincent JHS, Ni W, Blount JW, Jung HG, Masoud SA, Howles PA, Lamb C, Dixon RA. 1997. Reduced lignin content and altered lignin composition in transgenic tobacco down-regulated in expression of L-phenylalanine ammonia-lyase or cinnamate 4-hydroxylase. *Plant Physiology* 115: 41–50.
- Wang KLC, Li H, Ecker JR. 2002. Ethylene biosynthesis and signaling networks. *The Plant Cell* 18: 1931–1946.
- Weng JK, Mo H, Chapple C. 2010. Over-expression of F5H in COMT-deficient Arabidopsis leads to enrichment of an unusual lignin and disruption of pollen wall formation. *The Plant Journal* 64: 898–911.
- Yang WJ, Du YT, Zhou YB, Chen J, Xu ZS, Ma YZ, Chen M, Min DH. 2019. Overexpression of *TaCOMT* improves melatonin production and enhances drought tolerance in transgenic Arabidopsis. *International Journal of Molecular Sciences* 20: 652.
- Yao J, Sun D, Cen H, Xu H, Weng H, Yuan F, He Y. 2018. Phenotyping of *Arabidopsis* drought stress response using kinetic chlorophyll fluorescence and multicolor fluorescence imaging. *Frontiers in Plant Science* 9: 603.
- Zhang K, Cui H, Cao S, Yan L, Li M, Sun Y. 2019. Overexpression of *CrCOMT* from *Carex rigescens* increases salt stress and modulates melatonin synthesis in *Arabidopsis thaliana*. *Plant Cell Reports* 38: 1501–1514.
- Zhang KW, Qian Q, Huang ZJ, Wang YQ, Li M, Hong LL, Zeng DL, Gu MH, Chu CC, Cheng ZK. 2006. *GOLD HULL AND INTERNODE2* encodes a primarily multifunctional cinnamyl-alcohol dehydrogenase in rice1. *Plant Physiology* 140: 972–983.
- Zhao Q, Dixon RA. 2014. Altering the cell wall and its impact on plant disease: from forage to bioenergy. *Annual Review of Phytopathology* 52: 69–91.
- Zheng M, Jin C, Shi Y, Li Y, Yin Y, Yang D, Luo Y, Pang D, Xu X, Li W. 2017. Manipulation of lignin metabolism by plant densities and its relationship with lodging resistance in wheat. *Scientific Reports* 7: 41805.
- Zhu J, Mickelson SM, Kaeppler SM, Lynch JP. 2006. Detection of quantitative trait loci for seminal root traits in maize (*Zea mays* L.) seedlings grown under differential phosphorus levels. *Theoretical and Applied Genetics* 113: 1–10.

## Supporting Information

Additional Supporting Information may be found online in the Supporting Information section at the end of the article.

**Fig. S1** Maize *COMT* loss-of-function mutant (*brown midrib 3; bm3*) exhibits reduced lateral root density.

**Fig. S2** Pixel-based digital traits accurately represent plant biomass and shoot area in sorghum.

**Fig. S3** The fluorescence signature of sorghum *COMT* mutant, *bmr12* under well-watered conditions resembles the wild-type one under water-limited conditions.

**Fig. S4** Gas exchange properties of RTx430 (wild-type, WT) and sorghum *COMT* mutant, *bmr12* under well-watered (WW) and water-limited (WL) conditions.

**Fig. S5** Weighted gene co-expression network analysis (WGCNA) of RTx430 (wild-type, WT) and sorghum *COMT* mutant, *bmr12* root transcriptome under well-watered (WW) and water-limited (WL) conditions.

**Fig. S6** Effect of exogenous application of 1-aminocyclopropane-1-carboxylic acid (ACC) on shoot length, root length, lateral root density, and root to shoot length ratio in RTx430 (wild-type, WT) and sorghum *COMT* mutant, *bmr12* under well-watered conditions.

**Fig. S7** Effect of exogenous application of gibberellic acid (GA) inhibitor, daminozide (DMZ) on shoot length, root length, lateral root density, and root to shoot length ratio in RTx430 (wild-type, WT) and sorghum COMT mutant, and *bmr12* under well-watered conditions.

**Methods S1** Supplemental methods.

**Table S1** Phenotypic evaluation of RTx430 (wild-type, WT) and sorghum COMT mutant, *bmr12* and CAD mutant *bmr6* seedling root system.

**Table S2** Water holding capacity of wild-type (WT) and *bmr12* pots starting from the day water was withheld.

**Table S3** List of differentially expressed genes between wild-type and *bmr12* under well-watered and water-limited conditions.

**Table S4** List of genes in all the co-expression modules identified in weighted gene co-expression network analysis (WGCNA).

**Table S5** Normalized read counts for genes involved in GA catabolism in wild-type and *bmr12*.

Please note: Wiley Blackwell are not responsible for the content or functionality of any Supporting Information supplied by the authors. Any queries (other than missing material) should be directed to the *New Phytologist* Central Office.



## About *New Phytologist*

- *New Phytologist* is an electronic (online-only) journal owned by the New Phytologist Foundation, a **not-for-profit organization** dedicated to the promotion of plant science, facilitating projects from symposia to free access for our Tansley reviews and Tansley insights.
- Regular papers, Letters, Research reviews, Rapid reports and both Modelling/Theory and Methods papers are encouraged. We are committed to rapid processing, from online submission through to publication 'as ready' via *Early View* – our average time to decision is <26 days. There are **no page or colour charges** and a PDF version will be provided for each article.
- The journal is available online at Wiley Online Library. Visit **www.newphytologist.com** to search the articles and register for table of contents email alerts.
- If you have any questions, do get in touch with Central Office (np-centraloffice@lancaster.ac.uk) or, if it is more convenient, our USA Office (np-usaoffice@lancaster.ac.uk)
- For submission instructions, subscription and all the latest information visit **www.newphytologist.com**